An Inversion Algorithm for Retrieval of Atmospheric and Leaf Water Absorption From AVIRIS Radiance With Compensation for Atmospheric Scattering

Robert O. Green, James E. Conel, Jack S. Margolis,
Carol J. Bruegge, and Gordon L. Hoover

Jet Propulsion Laboratory
California Institute of Technology
Pasadena, California

Abstract. A radiative-transfer-based algorithm using a nonlinear least-squares fit for the retrieval of total atmospheric and leaf water abundance is described. This algorithm has been developed in pursuit of several objectives: (1) to study the distribution of atmospheric water vapor, which is an essential component of the hydrologic cycle; (2) to determine water vapor column abundance, which is required for the retrieval of surface reflectance from AVIRIS-measured radiance; and (3) to recover leaf water absorptions, which are important components of plant spectral signatures and can be confused with atmospheric water absorptions. The inversion algorithm operates on a nonlinear least-squares fit between the spectral radiance measured by AVIRIS and the spectral radiance calculated by a radiative transfer code. The algorithm generates parameters describing the surface reflectance, surface leaf water absorption, and atmospheric water vapor absorption. The residual error of the band fit and the number of iterations required to reach the solution are also reported. Factors of solar illumination geometry, surface pressure elevation, and atmospheric scattering are constrained and compensated for in the algorithm. Because combined atmospheric scattering and absorption are accounted for in the radiative transfer code, this algorithm allows an effective water vapor retrieval over surface water and dark targets where the upwelling radiance is derived dominantly from atmospheric scattering. Results from this algorithm are presented for an AVIRIS scene containing a healthy alfalfa field and a partially water-covered desert lake bed with in situ measurements of water vapor. For the water-saturated sediments of the lake bed, a liquid water absorption is identified and assessed. The accuracy and precision of this atmospheric and leaf water inversion algorithm are evaluated for these two examples.

1. Introduction

Atmospheric water vapor is a strong absorber across the AVIRIS spectral range, as shown in Figure 1, where spectra are presented with water vapor varying from 0 to 23.56 mm of precipitable water in the atmosphere. In addition to being a strong absorber, the amounts and distribution of the water vapor in the terrestrial atmosphere are highly variable. An example of spatial and temporal variation is given in Figure 2 [see slide 5], where water vapor was retrieved using a continuum interpolated band ratio of the 940-nm water band (Green et al., 1989) over four scenes of Rogers Dry Lake, California. Spatial variation is shown by gradients of 3 mm of precipitable water across this topographically featureless region. Temporal variation is demonstrated by the change in water vapor distribution through four images acquired at 12-min intervals.

Large variations in water vapor can also result from a change in the length of the atmospheric column due to change in surface elevation. For AVIRIS data acquired over the Ivanpah Valley at 800-m elevation and the Clark Mountains at 2000-m elevation, in southeastern California, a corresponding range of 22 to 8 mm of precipitable water vapor was retrieved (Green, 1991). Given the strength of the spectral absorption and the variability, water vapor must be accurately determined to allow the retrieval of surface reflectance from measured radiance over the AVIRIS spectral range. For vegetated areas, leaf water absorptions must be accounted for because of the overlap between the atmospheric and leaf water absorptions. Figure 3 shows these overlapping absorptions with a leaf spectrum superimposed upon a transmission spectrum for atmospheric water vapor. The overlap between the atmospheric and leaf water absorptions presents a challenge to the development of a robust retrieval algorithm. In addition, leaf water absorptions are of direct interest because they are important components of the spectral signature of vegetation.

2. Previous Work

Work on the recovery of water vapor from AVIRIS imaging spectroscopy data was originally pursued with ratios of radiance in and out of the 940-nm water band (Conel et al., 1988). These ratios were converted to precipitable water vapor using the LOWTRAN 7 (Kneizys et al., 1989) radiative transfer code. A continuum interpolated band-ratio algorithm calibrated against LOWTRAN 7 was developed to minimize the influence of change in surface reflectance with wavelength on the retrieval (Green et al., 1989). Calibration with LOWTRAN 7, which included compensation for atmospheric scattering, provided improved retrievals with typical atmospheric visibilities. An atmospheric and surface water band-fitting technique, based on an atmospheric water vapor and liquid water transmission model without compensation for atmospheric scattering, has also been developed and applied to AVIRIS data (Gao and Goetz, 1990). In addition, retrieval of terrestrial water vapor through the ratio of a wide and narrow filter centered at the 940-nm atmospheric water absorption without compensation for the asymmetric leaf water absorption has been described (Frouin and Middleton, 1990).

3. Atmospheric and Leaf Water Absorption Retrieval Algorithm

The present inversion algorithm for retrieval of atmospheric and leaf water uses a nonlinear least-squares fitting approach coupled with the MODTRAN (Berk et al., 1989) radiative transfer code. The radiative transfer code allows treatment of the atmosphere with compensation for (1) solar illumination and aircraft viewing geometries, (2) a seasonal and latitudinal atmospheric model, (3) atmospheric gaseous absorptions, and (4) molecular and aerosol scattering. In addition, the incorporation of a surface-reflectance model with the liquid water absorption of green vegetation addresses the asymmetrically overlapping absorptions of the atmospheric and leaf water.

AVIRIS measures the total upwelling radiance in nominally 10-nm spectral channels across the 940-nm atmospheric and 980-nm leaf water absorption bands. The inversion algorithm proceeds by establishing a nonlinear least-squares fit between AVIRIS-measured spectral radiance and radiative-transfer-code-modeled spectral

radiance, where the parameterized surface-spectral-reflectance function (including leaf water absorption) and the scaled atmospheric water vapor amount are allowed to vary. A computational routine applying the downhill simplex method for nonlinear least-squares fitting is applied (Nelder and Mead, 1965; and Press et al., 1986). The MODTRAN spectral radiance is calculated for each AVIRIS channel for a specific amount of atmospheric water vapor. The radiance is modeled as the total upwelling radiance, $L_t(H_2O_v)$, which results from a surface-reflected radiance, $L_r(H_2O_v)$, and an atmospheric-path-scattered radiance, $L_p(H_2O_v)$, as given in Equation 1:

$$L_t(H_2O_v) = L_r(H_2O_v) + L_p(H_2O_v) \quad (1)$$

The surface-reflected component of the radiance is described as the exoatmospheric solar irradiance multiplied by the cosine of the solar zenith angle over pi steradians, $E_s\cos\theta/\pi$, multiplied by the downward diffuse plus direct transmittance, T_d, surface lambertian reflectance, ρ, and upward diffuse plus direct transmittance, T_u, as in Equation 2:

$$L_r(H_2O_v) = [E_s\cos\theta/\pi]T_d\rho T_u \quad (2)$$

The surface reflectance is modeled as shown in Equation 3 as the sum of a reflectance offset, α, a reflectance slope, β, with respect to wavelength, λ, and a proportion, γ, of spectral leaf water absorption, H_2O_l.

$$\rho = \alpha + \beta\lambda + \gamma(H_2O_l) \quad (3)$$

The spectral region to which this algorithm applies is 850 to 1100 nm, which includes both the 940-nm atmospheric water band and the 980-nm leaf water absorption. The fit is performed with the 26 AVIRIS channels contained within this spectral region. The leaf water absorption spectrum $\alpha(\lambda)$ used for this algorithm is given in Figure 4. This spectrum was derived by normalization of a laboratory-measured alfalfa-leaf spectrum across the 980-nm water absorption region and is scaled by a factor γ.

MODTRAN is initialized with the solar illumination geometry appropriate for the AVIRIS data set. An atmospheric model is selected based on the location and season of the AVIRIS acquisition. Atmospheric-scattering properties are constrained by scaling the atmospheric model to in situ measurements of the optical depth or estimates of the visibility. In the presence of significant topographic relief, the optical depths are extrapolated across the AVIRIS scene through modulation with estimates of the surface pressure elevation derived from the absorption of carbon dioxide or oxygen measured within the AVIRIS spectrum.

The inversion algorithm operates on the spectrum of each AVIRIS spatial element and generates images of the fit parameters of reflectance offset, reflectance slope, leaf water absorption, and abundance of atmospheric water vapor. In addition, images of the root-sum-squared (RSS) residual radiance in the fit and the number of iterations required to achieve the fit are generated.

4. AVIRIS Radiance Inversion for Atmospheric and Leaf Water

This inversion algorithm has been evaluated with an AVIRIS radiance image over a portion of Mesquite Valley, California. This scene contains desert surface cover, as well as heavily vegetated fields of alfalfa grown under pivot irrigation. These data were acquired on July 23, 1990. Figure 5 shows a radiance image of the Mesquite Valley scene. The algorithm was constrained with the solar illumination geometry, in situ measurements of atmospheric optical depth, a rural midlatitude summer atmospheric model, and an estimate of the mean elevation of the scene. The optical depths were measured at a site 40 km to the south, at approximately the same elevation. At 400 nm, the total optical depth was 0.4, indicating minimal aerosol scattering. In Figure 6 [slide 6], the results of the inversion algorithm are presented. From upper left to lower right, the images correspond to the parameters of reflectance offset, reflectance slope, leaf water absorption, atmospheric water amount, RSS residual radiance, and a number of iterations required for the fit. In parameter images 3 and 4, the surface leaf water and atmospheric water vapor are successfully separated with no confusion between the leaf and atmospheric water over the alfalfa fields. Figure 7 gives a comparison of the AVIRIS-measured radiance spectrum and the inversion algorithm fit for a spectrum from the alfalfa field. The residual between these two spectra is given in Figure 8. The reflectance spectrum determined by the algorithm to achieve this fit is given in Figure 9. The presence of leaf water absorption in this spectrum is consistent with the presence of healthy alfalfa at the surface.

To further evaluate this atmospheric and leaf water inversion algorithm, an AVIRIS data set acquired over the Ivanpah Playa, on March 7, 1991, has been examined. A radiance image of the Ivanpah site is given in Figure 10. At the time of acquisition, a portion of the playa surface was inundated by water and represented a dark target at 940 nm. The algorithm was constrained with solar geometry, in situ optical-depth measurements, an appropriate atmospheric model, and mean surface elevation. The optical-depth measurements were acquired concurrently with the AVIRIS data at a site just above the oval feature on the playa. At 400 nm, the total optical depth was less than 0.4 throughout the day (visibility = 300 km). Figure 11 presents the results from the inversion algorithm. From the water vapor parameter image, a value of 3.5 mm of precipitable water vapor was retrieved for the site on the playa. An independent determination of water vapor was generated from sun photometer measurements at this site using a spectrally based retrieval algorithm (Bruegge et al., 1990). This determination produced a value of 3.7 ± 0.2 mm of water vapor at about 19:30 UCT when the AVIRIS data were acquired.

The algorithm was further evaluated for retrieval of water vapor over surface water by examining the results obtained over the inundated portion of the playa. This water vapor parameter image displays no observable boundary effects caused by the transition from the bright playa to the dark water surface implying that the method successfully compensates for spectral surface reflectance changes. Consistent retrieval of water vapor over this dark water surface results from the inclusion of a combined treatment of gaseous absorption and atmospheric scattering in the algorithm. For such targets, atmospheric-scattered-path radiance dominates the upwelling radiance measured by AVIRIS. Also associated with the inundated portion of the playa is a region of water-saturated playa sediment. These saturated sediments

exhibit a liquid water absorption analogous to the leaf water, which is partitioned into the leaf water parameter image by the inversion algorithm. Figure 12 presents the laboratory reflectance spectrum for dry and water-saturated sediment from the Ivanpah Playa. This inversion algorithm generates consistent water vapor and leaf water results over vegetated and unvegetated surfaces, as well as dark surfaces and water-saturated sediments.

5. Error Discussion

Validity of the reflectance model and radiative transfer code is a factor that directly influences the accuracy of the atmospheric and leaf water retrievals. Constraints of the input parameters of the radiative transfer code, particularly on atmospheric scattering and the spatial variation of scattering, affect the retrieval. The accuracy of atmospheric and leaf water retrieval will also be influenced by the absolute radiometric calibration of the AVIRIS sensor. The radiometric accuracy of AVIRIS is traced to the laboratory calibration (Chrien et al., 1990) and validated through periodic in-flight calibration experiments (Green et al., 1990).

To evaluate the character and accuracy of the fit between the AVIRIS-measured radiance and the MODTRAN-calculated radiance, the residual RSS error and the number of iterations to achieve the fit are reported. These parameters provide a rapid evaluation of the quality of the fit, and analysis of these images allows further refinement of this inversion algorithm.

Absolute accuracy of this algorithm is currently validated solely at the Ivanpah Playa site where in situ water vapor measurements were acquired. Additional AVIRIS scenes with in situ measurements have been identified for continued validation analysis.

Within each AVIRIS scene, the precision of water vapor retrieval will be a function of the sensor performance, solar illumination, surface reflectance, and amount of water vapor. To estimate the precision of the retrievals, a statistical method is adopted. This method proceeds by calculating the root-mean-squared deviation (RMSD) of all possible 5 by 5 spatial-element regions within the water vapor image. The lowest calculated RMSD is reported as an estimate of the water vapor retrieval precision. This lowest RMSD corresponds to the most homogeneous portion of the water vapor image, where instrument noise should represent the dominant contributor to variability. This is a worst-case estimate of the precision because any residual variability in water vapor within the 5 by 5 area is included in this precision estimate. For the Mesquite Valley scene, a precision of ±0.3 for 15.4 mm of water vapor was estimated. The Ivanpah Playa scene acquired under the winter-illumination condition yielded a precision estimate of ±0.2 for 3.4 mm of water vapor. These precision estimates are determined at the full AVIRIS spatial resolution and may be improved by spatial averaging of the data.

6. Conclusion

An inversion algorithm for retrieval of atmospheric water vapor and surface leaf water absorption from AVIRIS-measured radiance has been developed. This algorithm is

based on a nonlinear least-squares fit between an AVIRIS radiance spectrum and a radiative-transfer-code-modeled spectrum. For each spatial resolution element of the AVIRIS image, the parameters generated by the algorithm are reflectance offset, reflectance slope with respect to wavelength, surface leaf water absorption, and atmospheric water vapor absorption. Inclusion of atmospheric-scattered radiance in the MODTRAN radiative transfer code and the combined treatment of gas absorption and scattering allow retrievals over dark targets such as surface water. This algorithm has been applied to two AVIRIS scenes. The first scene of the Mesquite Valley region contains extreme contrasts in surface vegetation cover. Both atmospheric water and leaf water absorptions are retrieved by the algorithm in a manner consistent with the distribution of surface cover. A second AVIRIS scene of the Ivanpah Playa, California region was examined with the algorithm. For this image, a good agreement was obtained with in situ column water vapor measurements. In addition, water vapor was retrieved successfully over an inundated portion of the playa. This inversion algorithm has applications towards the objectives of direct study of water vapor, compensation for water vapor in the retrieval of reflectance, and study of plant spectral signatures. Future work will be directed towards further validation of absolute accuracies of the retrieval, as well as refinement of estimation of the retrieval precisions. Issues associated with the accuracy of the radiative transfer code itself with emphasis on the treatment of atmospheric scattering will also be investigated.

Acknowledgment

This research was carried out at the Jet Propulsion Laboratory, California Institute of Technology, under contract with the National Aeronautics and Space Administration.

References

Berk, A., L. S. Bernstein, and D. C. Roberson, "MODTRAN: A Moderate Resolution Model for LOWTRAN 7," U.S. Air Force Geophysical Laboratory, Hanscom Air Force Base, Massachusetts, 1989.

Bruegge, C. J., J. E. Conel, J. S. Margolis, R. O. Green, G. Toon, V. Carrere, R. G. Holm, and G. Hoover, "In-Situ Atmospheric Water Vapor Retrieval in Support of AVIRIS Validation," *Imaging Spectroscopy of the Terrestrial Environment*, SPIE Vol. 1298, 1990.

Chrien, T. G., R. O. Green, and M. Eastwood, "Laboratory Spectral and Radiometric Calibration of the Airborne Visible/Infrared Imaging Spectrometer (AVIRIS)," *Imaging Spectroscopy of the Terrestrial Environment*, SPIE Vol. 1298, 1990.

Conel, J. E., R. O. Green, V. Carrere, J. S. Margolis, R. E. Alley, G. Vane, C. J. Bruegge, and B. L. Gary, "Atmospheric Water Mapping With the Airborne Visible/Infrared Imaging Spectrometer (AVIRIS), Mountain Pass, CA," *Proceedings of the AVIRIS Performance Evaluation Workshop* (G. Vane, ed.), JPL Publication 88-38, Jet Propulsion Laboratory, Pasadena, California, pp. 21–26, 1988.

Frouin, R., and E. Middleton, *Proceedings of AMS Symposium on FIFE*, 70th AMS Annual Meeting, Anaheim, California, pp. 135–139, 1990.

Gao, B.-C., and A. F. H. Goetz, "Column Atmospheric Water Vapor and Vegetation Liquid Water Retrievals From Airborne Imaging Spectrometer Data," *J. Geophys. Res.*, Vol. 95, pp. 3549–3564, 1990.

Green, R. O., V. Carrere, and J. E. Conel, "Measurement of Atmospheric Water Vapor Using the Airborne Visible/Infrared Imaging Spectrometer," *Image Processing '89*, American Society for Programmetry and Remote Sensing (ASPRS), 1989.

Green, R. O., J. E. Conel, J. S. Margolis, V. Carrere, C. J. Bruegge, M. Rast, and G. Hoover, "In-Flight Validation and Calibration of the Spectral and Radiometric Characteristics of the Airborne Visible/Infrared Imaging Spectrometer (AVIRIS)," *Imaging Spectroscopy of the Terrestrial Environment*, SPIE Vol. 1298, 1990.

Green, R. O., "Retrieval of Reflectance From AVIRIS-Measured Radiance Using a Radiative Transfer Code," *Proceedings of the Third Airborne Visible/infrared Imaging Spectrometer (AVIRIS) Workshop*, JPL Publication 91-28, Jet Propulsion Laboratory, Pasadena, California, 1991 (this publication).

Kneizys, F. X., E. P. Shettle, G. P. Anderson, L. W. Abrew, J. H. Chetwynd, J. E. A. Shelby, and W. O. Gallery, "Atmospheric Transmittance/Radiance: Computer Code LOWTRAN 7," U.S. Air Force Geophysical Laboratory, Hanscom Air Force Base, Massachusetts, 1989.

Nelder, J. A., and R. Mead, *Computer Journal*, Vol. 7, p. 308, 1965.

Press, W. H., B. P. Flannery, S. A. Teukolsky, and W. T. Vetterling, *Numerical Recipes*, Cambridge University Press, 1986.

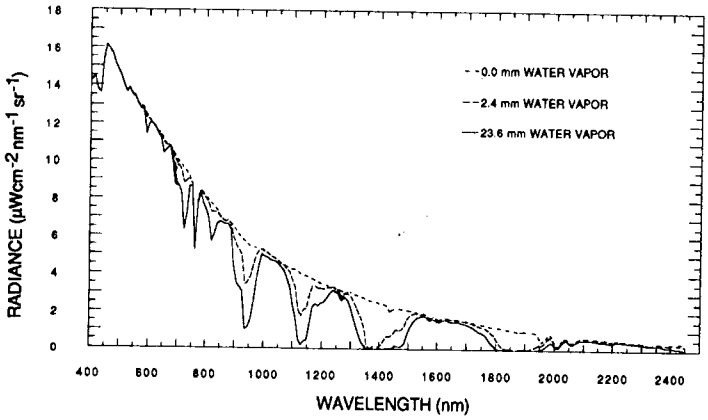

Figure 1. Water vapor absorption over the AVIRIS spectral range, modeled by MODTRAN as the total-column precipitable water varies from 0 to 23 mm.

Figure 2. Water vapor retrieved for four consecutive overflights of the Rogers Dry Lake, California calibration site. Both patchiness in water vapor and change in water vapor through time are shown.

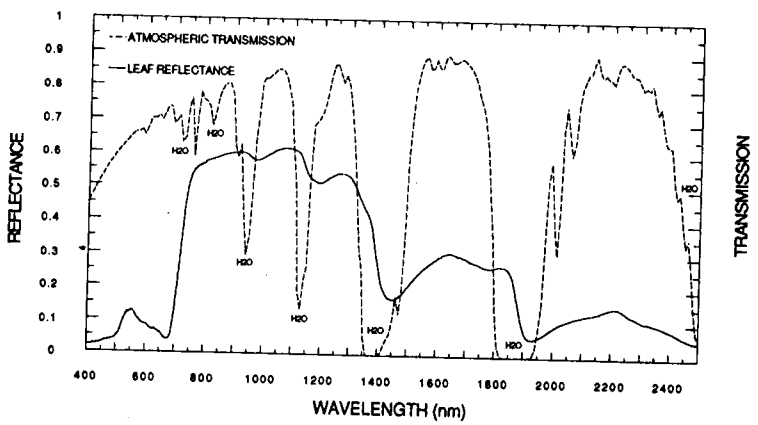

Figure 3. Laboratory reflectance spectrum of alfalfa leaves with the atmospheric transmission for water vapor superimposed. These spectra show the overlap between the atmospheric water vapor and leaf water absorptions.

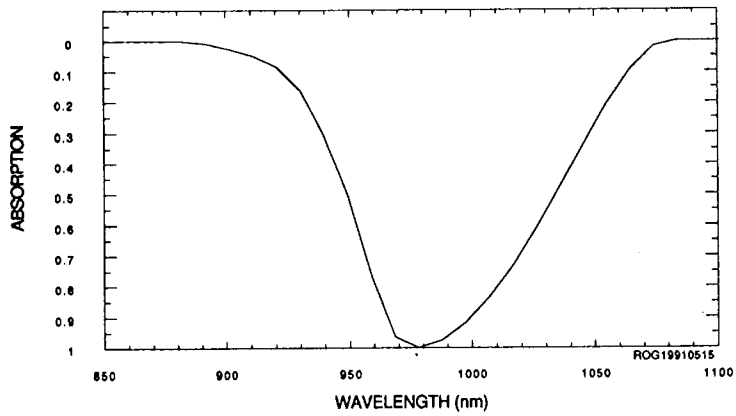

Figure 4. Normalized leaf water absorption spectrum used in the inversion algorithm.

Figure 5. An AVIRIS image of pivot irrigation field of alfalfa in Mesquite Valley, California. These data were acquired on July 23, 1990. The scene center is at 35 deg, 48.3 min north latitude, and 115 deg, 41.7 min west longitude.

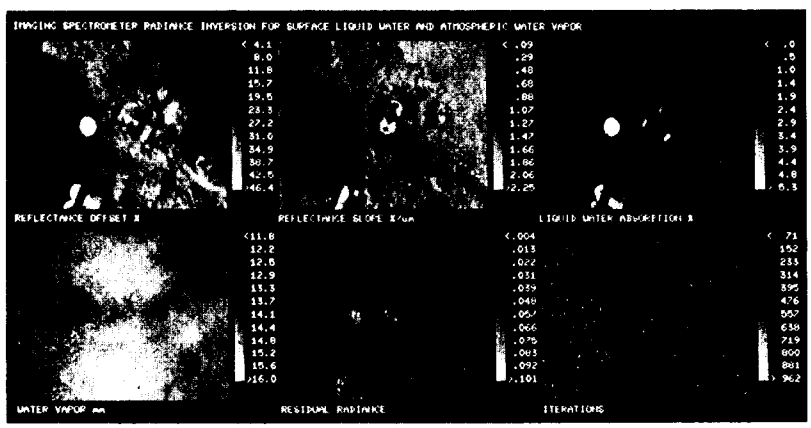

Figure 6. Retrieval of leaf and atmospheric water vapor for pivot alfalfa fields from AVIRIS-measured radiance. Top row: retrieved reflectance offset, reflectance slope, and leaf water. Bottom row: retrieved atmospheric water, residual error, and number of iterations for solution.

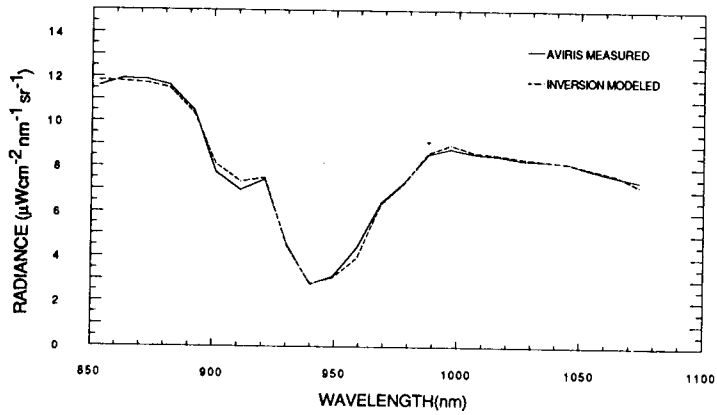

Figure 7. Result for the alfalfa field presenting the AVIRIS-measured radiance spectrum and the inversion-algorithm-calculated radiance spectrum.

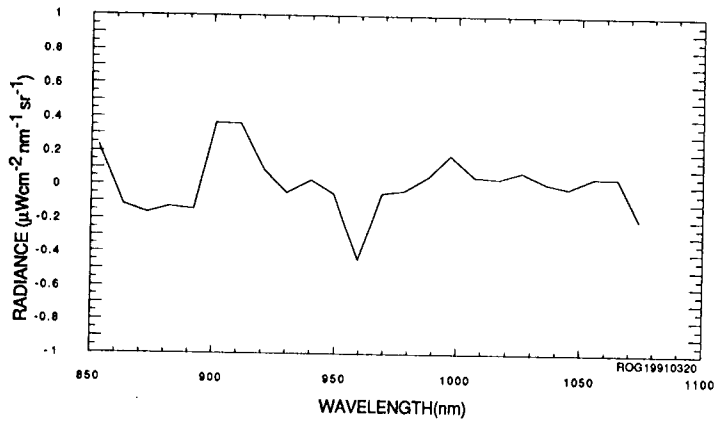

Figure 8. Radiance residual for the central alfalfa field following application of the inversion algorithm.

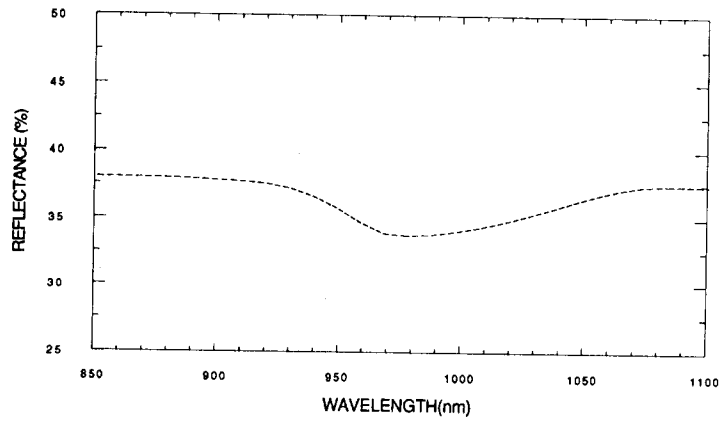

Figure 9. Reflectance spectrum determined by the nonlinear least-squares fitting algorithm for the central alfalfa field. As expected the surface leaf water absorption is recovered.

Figure 10. AVIRIS image of the Ivanpah Playa, California. A portion of the playa is inundated with water. Regions of water-saturated playa soil are found adjacent to the standing water.

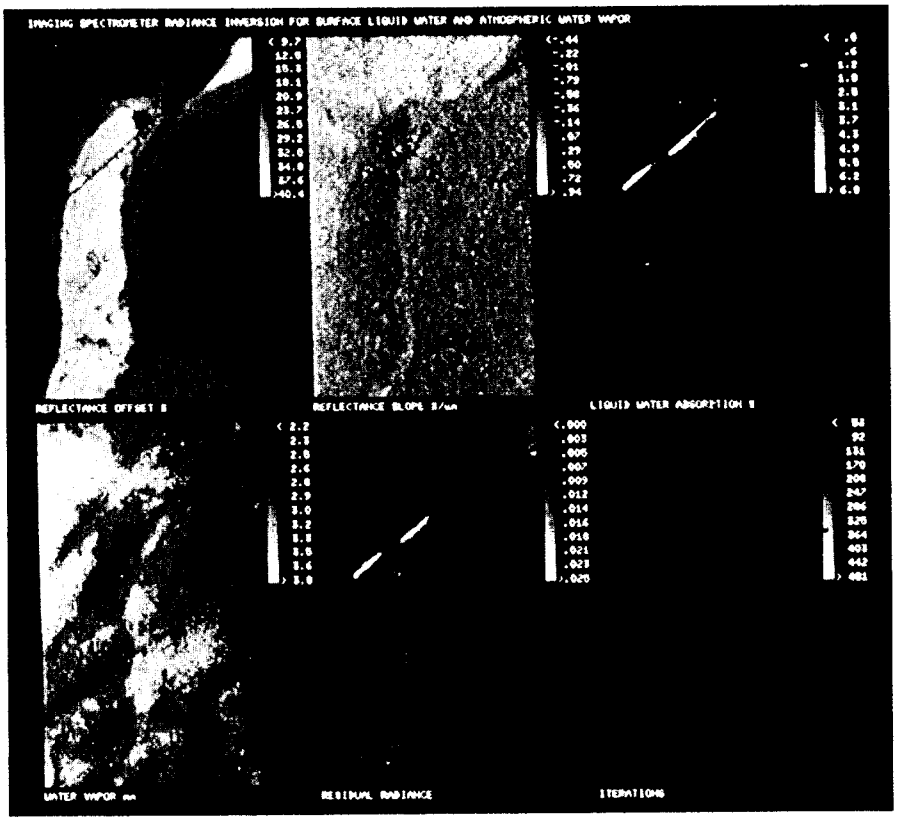

Figure 11. Atmospheric water vapor retrieval for the Ivanpah Playa AVIRIS radiance imagery. Water vapor is successfully retrieved over the standing water and regions of water-saturated playa soil. The saturation soil is isolated based on the presence of liquid water absorption features.

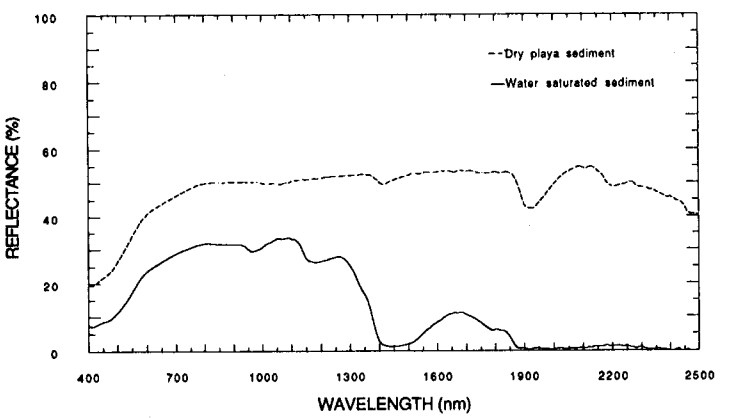

Figure 12. Reflectance spectrum of dry sediment from the Ivanpah Playa and a spectrum of water-saturated sediment. These data were acquired by a laboratory spectrometer and convolved the AVIRIS spectral characteristics.